Wavelet transform processing applied to partial discharge evaluation

2012 J. Phys.: Conf. Ser. 364 012054

(http://iopscience.iop.org/1742-6596/364/1/012054)

Journal of Physics: Conference Series **364** (2012) 012054 doi:10.1088/1742-6596/364/1/012054

Wavelet transform processing applied to partial discharge evaluation

E C T Macedo[1,2], D B Araújo[2], E G da Costa[2], R C S Freire[2], W T A Lopes[2], I S M Torres[2], J M R de Souza Neto[2], S A Bhatti[3] and I A Glover[3]

[1] Alternative and Renewable Energy Center, Paraíba Federal University - UFPB, João Pessoa, Brazil.
[2] Electrical Engineering and Informatic Center, Campina Grande Federal University - UFCG, Campina Grande, Brazil.
[3] Department of Electronic and Electrical Engineering, University of Strathclyde, Scotland, UK.

E-mail: euler@cear.ufpb.br and ian.glover@eee.strath.ac.uk

Abstract. Partial Discharge (PD) is characterized by high frequency current pulses that occur in high voltage (HV) electrical equipments originated from gas ionization process when damaged insulation is submitted to high values of electric field [1]. PD monitoring is a useful method of assessing the aging degree of the insulation, manufacturing defects or chemical/mechanical damage. Many sources of noise (e.g. radio transmissions, commutator noise from rotating machines, power electronics switching circuits, corona discharge, etc.) can directly affect the PD estimation. Among the many mathematical techniques that can be applied to de-noise PD signals, the wavelet transform is one of the most powerful. It can simultaneously supply information about the pulse occurrence, time and pulse spectrum, and also de-noise in-field measured PD signals. In this paper is described the application of wavelet transform in the suppression of the main types of noise that can affect the observation and analysis of PD signals in high voltage apparatus. In addition, is presented a study that indicates the appropriated mother-wavelet for this application based on the cross-correlation factor.

1. Introduction

Electrical insulation constitutes a very critical component of HV power apparatus. In spite of advances in manufacturing areas, processing, optimal design and quality control, these apparatus have continued to fail while in service. Investigations reveal that, in most cases, the insulation is the primary cause. Due of this, power utilities are increasingly resorting to diagnostic measurements to assess the status of the insulation system. Amongst others, PD measurements have emerged as an indispensable, non-destructive, sensitive and powerful diagnostic tool. Using this diagnostic data, an overall assessment of the insulation system is possible [2].

PD are normally low-level current pulses with fast rise-time and short duration, typically no more than a few hundred nanoseconds. Its waveform varies depending on the fault type, PD detection sensor, insulation characteristics and physical connection [3].

Increases in PD sensor sensitivity, decreases in sensor costs and increasingly cheap analog-to-digital conversion and digital signal processing are some of the reasons for the increase in

popularity of automated insulation condition diagnosis systems [4]. Such systems often rely on the analysis of PD signals.

However, the analysis of PD measurements in the field is often hampered by electrical noise, which need the application of sophisticated digital signal processing techniques.

In accordance with [4], the ability to discriminate PD signals from the noise increases with the knowledge of the PD signal and noise characteristics. Based on this argument, in the Section 2 are presented the basics concepts that concern the PD phenomena. Some of the main techniques used to perform the PD detection and measurement are presented in Section 3, and in the Section 4, are presented the most common types of interference that can prejudice in-field and laboratory PD measurement.

2. Partial discharge concepts

In accordance with the IEC standard [3], the PD can be defined as localized electric discharges that partially short circuit the insulation between conductors and can or not occur in the conductor surroundings. Also in accordance with the standard, a PD pulse can be defined as a voltage or current pulse obtained in a specific device under test (DUT).

The partial discharges are extremely harmful for the dielectric and also for the HV equipment. It can generate heat, oxidating agents as ozone, electromagnetic waves, that cause radio-receptions interferences and can cause the insulation deterioration [1]. Depending on the discharges intensities the insulation material useful life can be reduced.

Based on these information's, PD measurement and analysis allows the HV insulation quality evaluation, and in consequence, increase the performance of the HV substations. The unit commonly used to quantify the partial discharges is the picocoulomb (pC).

PD can occur in any point of the dielectric material, e.g., in the junction of two different dielectric materials, in the electrode adjacent regions, and in some points of the material or only in a dielectric void, as presented in the Figure 1.

Moreover, PD pulses presents a short duration (nanoseconds) in relation to the applied sinusoid voltage period, they are repetitive and have a very short rise time, being able to be modeled as an ideal impulse function $\delta(t)$.

The Figure 2 will be used to briefly explain the formation process of a PD. Consider initially that an alternated voltage U_t(t) is applied to a DUT insulation material with a unique void. When the voltage U_t(t) reaches the value of U+, occurs a discharge in the void reducing the voltage for a V+ value. The phenomena can be repeated several times during each applied voltage cycle. The discharge duration is in order of 10^{-7}s, a very small time when compared with the applied voltage period. Being U(t) the waveform of the resultant voltage in the void, U+ and U- are the void disruptive voltage, i.e., the voltage levels which the PD occur, and V+ and V- are denominated residual voltages in the void after the discharge, and they possess a non-zero value.

3. Partial discharge measurement methods

PD generates both physical (including electrical, acoustic and optical phenomena) and chemical phenomena (gas ionization). Popular techniques for PD detection include the electrical configurations presented in the IEC 60270 standard [3], acoustic emission based methods [5], ultra high frequency (UHF) measurements [6], high frequency inductive current transformers (HFCT) sensors [7], and radiometric systems [8].

The measurement techniques presented in IEC 60270 are often used to evaluate PD in controlled areas, such as laboratories. The measurement techniques usually integrates the PD pulses with an oscillation frequency (hundreds of kHz), and generally are exposed to the environment interferences (RF, white noise, periodic pulse-shape noise from power electronics switching).

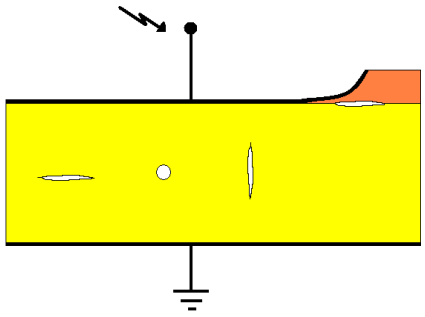

Figure 1. Example of insulation defects that can cause PD.

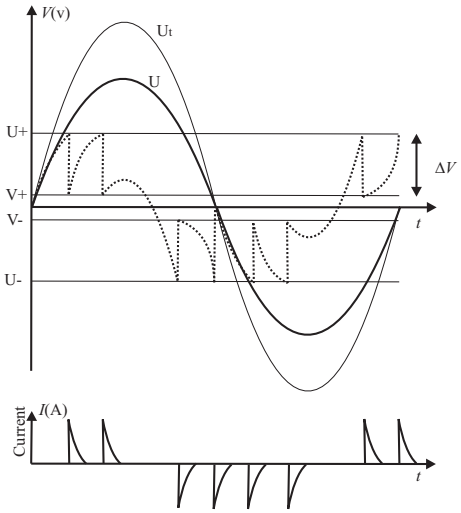

Figure 2. Partial discharge formation process representation.

An acoustic measurement of PD activity relies in the detection of a wave that occurs in the HV equipment insulation when a PD pulse occurs. In this case, the pulse shape of the signals associated with PD (90 - 250 kHz) provides limited information about the PD occurring.

The UHF PD detection has been used to detector and monitor PD pulses allocated in the frequency range of 300 MHz and 3 GHz. The UHF PD detection systems are also vulnerable to environment interferences, specially the discrete spectral interference (DSI) arising from radio-transmissions. Other technique widely used in field and laboratory PD measurements is the use of HFCT, and in some cases presents a wide-band frequency range (10 kHz - 1.75 GHz). The HFCT measurements are also exposed to noise, especially radio-frequency (RF) and pulsive shaped noise, but presents an easier installation and present satisfactory results when compared to PD measurement techniques based on the IEC 60270 standard. Another measurement possibility is the technique based on free-space radiometric method, that can detect PD processes remotely, and it can be implemented using low-cost antennas and this technique is capable to detect PD pulses in the same frequency range of the UHF techniques, i.e. (300 MHz -3 GHz).

3.1. Electrical partial discharge measurement

The electric pulses detection caused by the PD is one of the most popular methods and exist a significant variety of circuits used to its detection. The classical detection of PD is described in [3]. The basic standard model is illustrated schematically in Figure 3.

Where in accordance with [3], $U \sim$ is a high-voltage power supply, Z_{mi} is the input impedance of the measuring system, CC is the connecting cable, C_a is the device under test, C_k is the coupling capacitor, CD the coupling device and MI is the measuring instrument.

The coupling capacitor allows the flow only of the short PD current pulses, increasing the measurement sensitivity. The measurement impedance converts the PD current pulses to a proportional voltage for convenient amplification, visualization (using, a high acquisition-rate oscilloscope), measurement and storage.

The electrical PD measurement is commonly used in generators, transformers, HV cables, capacitors, etc. The coupling device CD can be implemented by a RLC (resistor, inductor and capacitor) circuit or a RC circuit (resistor and capacitor). The RLC circuit is used in narrow-band detection and the RC circuit is used wide-band mode detections. The schematic

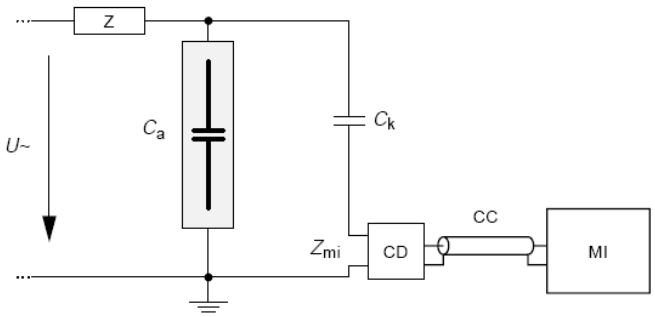

Figure 3. Standard setup used for PD measurement [3].

representation of the coupling devices configurations are presented in Figure 4.

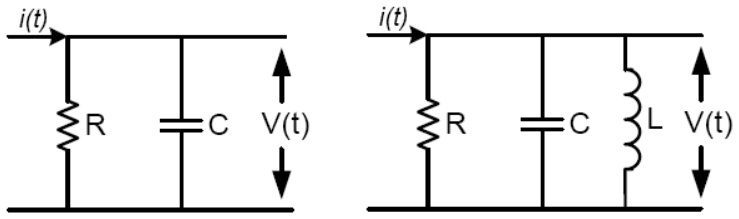

Figure 4. PD measurement coupling device configurations: (a) RC e (b) RLC.

The narrow-band measurement circuit posses a superior immunity to external noises, therefore it can be tuned to a frequency band that minimizes the narrow-band interferences effect, e.g., the AM/FM transmissions and others. However, narrow-band measurement circuits can cause measurement errors due to the integration effect (overlapping) of the PD pulse, when several pulses occur simultaneously [9].

In accordance with [9], if an ideal step voltage is the input of the measurement circuits presented in Figure 4, the output signal $V(t)$ of the RC circuit is a damped exponential pulse (DEP), as denoted by Equation (1).

$$V(t) = A(e^{\frac{-t}{t_1}} - e^{\frac{-t}{t_2}}).u(t) \tag{1}$$

Considering the situation where the PD measurement is performed with a RCL coupling device, and the same ideal step voltage is used as input voltage, in the coupling device output is obtained a damped oscillatory pulse (DOP), described by the Equation (2).

$$V(t) = A\sin(2\pi f_c t)(e^{\frac{-t}{t_1}} - e^{\frac{-t}{t_2}}).u(t), \tag{2}$$

where A is the pulse peak value, t_1 and t_2 the time constants that determine the PD pulse typical parameters, such as, rise time, pulse width and fall time. The parameter f_c is the DOP oscillatory frequency, in accordance with Equation (2) [10].

3.2. HFCT partial discharge measurement

The PD measurement diagram using an HFCT is illustrated in Figure 5. The HFCT is usually connected in series with the DUT ground connection, since using this configuration the personal

safety is increased.

The HCFT used in this work has a rise-time inferior to 175 ps and a high frequency -3 dB cutoff of 2 GHz. The HFCT output is a current flowing in a 50 Ω load. The core is a composite of CoFe amorphous alloy and nanocrystalline alloy to optimize the frequency response and minimize ringing. The CoFe alloy is cross-field annealed for this application.

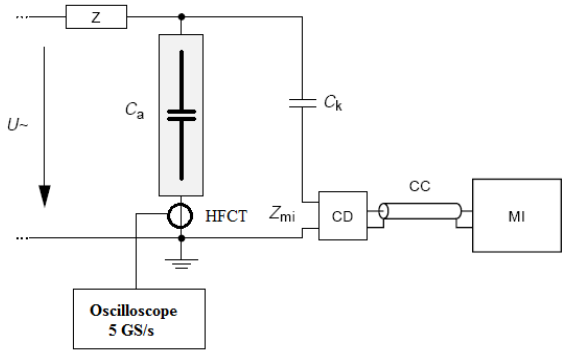

Figure 5. Standard setup used for PD measurement [3].

As presented in the Section 1, one of the main difficulties in perform the PD measurement in-field and in laboratory is its susceptibility to electromagnetic interferences (EMI) that can exist in the measurement environment (usually of very high amplitude when comparable to PD signal), this characteristic can directly affect the PD measurements sensitivity. Some details about these interferences and some techniques used for its removal are presented in the sequence.

4. Interferences that affect the PD measurement

In the majority of the PD measurements, the external interferences can cause a wrong indication in the PD measured signals analysis, reducing the PD measurements credibility. In accordance with [9], [2],[10], any or all of the following effects can prejudice the PD measurements:

- Discrete spectral interference (DSI), e.g. communication and amplitude modulation (AM) and frequency modulation (FM) radio emissions;
- Repetitive pulses, e.g. from power electronics;
- Random pulses, e.g.from switching operations, lightning or RF corona emitted from HV equipment;
- Other noise sources such as ambient and amplifier noise.

In terms of its nature, the noise can be classified as sinusoidal noise (DSI), pulsive type noise (repetitive and random noise), white noise (amplifier and ambient noise). DSI is a narrow band noise signal, the other types of noise are wide-band signals [11].

Random pulse interference is the most common interference source and presents the biggest problem to on-line PD measurements. The pulse frequency characteristics are quite similar to PD signals and need an advanced filtering technique to separate the PD from random noise pulses [12].

In the sequence, some of the main techniques used for noise rejection or interferences attenuation are presented.

5. Noise rejection techniques applied to PD measurements

Much recent effort has been dedicated to the development of computational methods to suppress external noise and interference that contaminate on-line PD signals measurements with the objective of increasing PD measurement sensitivity [12].

Some authors developed computational techniques based on Fast Fourier Transforms (FFT), however, these techniques presents a high computational requirements [13]. Techniques based on adaptive filters were developed as well. This approach have presented some limitations related to the desired remove noise level. Others techniques based on predictive and Kalman filters were developed, but presented limited results when applied to PD signals measured in-field [14].

The most common techniques used to remove, or suppress noise of non-PD origin work in either the time domain or the frequency domain. When the signal is processed in only one domain, the information relating to the other domain is lost or degraded.

The Wavelet transform is a different approach that allows multi-resolution analysis [9], i.e., implementing processing simultaneously in both domains. Several authors had presented the use of the Wavelet transform to perform the analysis and de-noise of PD signals. Some main publications related to this approach are presented by: [4], [9], [2], [15], [16], [17], [10], [16], [18] and [19].

The majority of the presented techniques generally perform the removal of DSI interferences and usually presents satisfactory results for this type of interference. Currently, it was verified that the main problem related with the PD measurement is related with the suppression or removal of pulsive type interferences.

After a simplified bibliographical review, was evident that the PD signal analysis and de-noise using wavelet transform have been presented as an interesting possibility when compared with the existing techniques related to PD signals noise suppression. In the sequence is presented a concise review about the Wavelet transform.

5.1. The Wavelet transform

The Wavelet transform is a signal processing computational tool that can be useful in the elaboration of an alternative signals representation [20]. The discrete Wavelet transform allows a multi-resolution signal analysis, that can be mathematically expressed by the Equation (3).

$$f(t) = \sum_{k=-\infty}^{\infty} c(k).\varphi_k(t) + \sum_{j=0}^{\infty}\sum_{k=-\infty}^{\infty} d(j,k).\psi_{j,k}(t) \tag{3}$$

Where $\varphi_k(t)$ and $\psi_{j,k}(t)$ are obtained respectively, from the scale function $\varphi(t)$ and from the mother-wavelet $\psi(t)$, as presented by the Equations (4) and (5).

$$\varphi_k(t) = \varphi(t-k) \tag{4}$$

$$\psi_{j,k}(t) = 2^{j/2}.\psi(2^j.t-k) \tag{5}$$

The coefficients $c(j)$ represents the approximation information of the original signal, while the coefficients $d(j,k)$ represent the details information of the original signal. One of the biggest advantages of the multi-resolution analysis is its computational simplicity for the calculation of the coefficients $c(j)$ and $d(j,k)$. The scheme for the coefficients calculation is shown in the Figure 6.

After the multi-resolution analysis, the noise attenuation consists of zeroing the coefficients that are related to the noise, and finally reconstructing the signal performing the inverse discrete Wavelet transform (IDWT). The recovery process involves the operation *up-sampling*, that it is inverse process of the *down-sampling*. In a numbers sequence, between two consecutive numbers, a zero value is inserted.

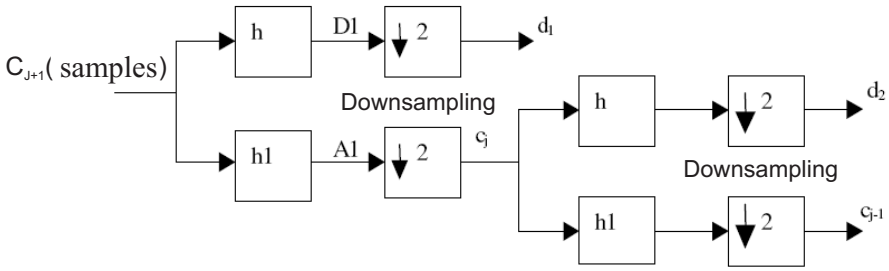

Figure 6. Three stages Wavelet decomposing structure.

The noise attenuation is performed submitting each coefficient to a threshold value. The threshold can be divided in *hard-threshold* and *soft-threshold*:

- The hard-threshold consists in make zero all the coefficients that are below the threshold;
- The soft-threshold consists in multiply all the coeficientes by a reduction factor.

In accordance with [20], the coefficients contained in the vector c_{j+1} are obtained from the signal to be analyzed sampling. From the vector coefficients c_{j+1}, the wavelets coefficients from the family "d_j" can be calculated using the structure presented in the Figure 6.

Each filter stage has as input the coefficients of the scale function and the output coefficients of the *wavelet* and scale functions in a lower resolution. The structure is a filter bank because h and $h1$ are respectively high-pass and low-pass digital filters [18]. It means, in the Figure 6, $A1$ is the vector that contains the signal approximation c_{j+1} in the first resolution level. The *down-sampling* makes possible that the output formed by the vectores c_j and d_1 addition has the same length of the sampled signal, because it consists in the selection and transforming of a number sequence [21]. The new selection will be composed by the previous number sequence except the even sequence numbers. This filters bank structure makes easy the coefficients calculation and allow the analyze of the signal in different resolution levels.

In the sequence will be presented the methodology used in the simulations and measurements of the PD signals, starting by the main PD interferences simulations, and the developed wavelet transform characteristics. In the end the results will be analyzed using different criteria.

6. Simulations and measurement methodology

In this section, will be described the simulation of the PD pulses and the main types of interference.

6.1. PD pulses and noise simulation

6.1.1. PD pulses simulation. Based on the Equations (1) and (2), were simulated using the Matlab© computational environment, the PD pulse measurement using the two different coupling device configurations. The simulations results are presented in Figures 7 and 8.

As presented in the Section 2, it was verified that the occurrence of PD pulses is related to the applied voltage cycle phase in relation to the insulation defect type. It was verified that the PD pulses occur when the time-derivative of the electrical field is intense. As presented, generally the PD appears in a train of pulses form (see Figure 2). The simulated train of pulse can be visualized in the Figure 9.

In the sequence are presented the main characteristics of the most common interferences found in laboratory and in-field measurements.

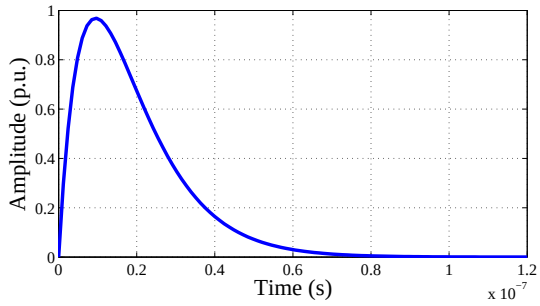

Figure 7. Typical PD pulse measured with a RC coupling device.

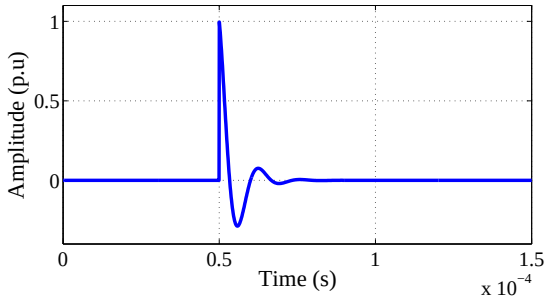

Figure 8. Typical PD pulse measured with a RLC coupling device.

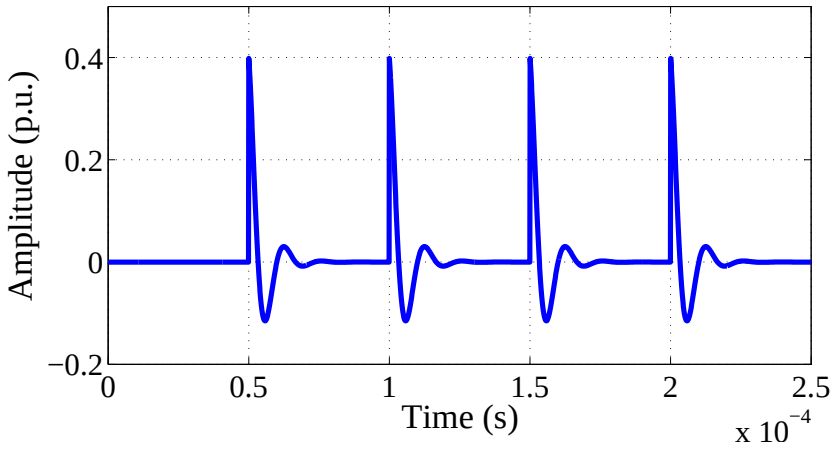

Figure 9. Train of pulses measured in a RLC impedance simulation.

6.1.2. DSI - Discrete spectral interference simulation. Generally in radio communications, a numerous number of transmission systems are based in amplitude (AM) and frequency (FM) modulation, each modulation type posses a specific operation frequency range [22].

Considering the FM transmissions frequency range, it was verified that this type of communication does not have a great influence in the PD measurements and will not be considered in this paper. Only the influence caused AM modulations will be studied.

Based in the knowledge that the AM commercial communication is allocated in the frequency range of 530 - 1700 kHz, a combination of amplitude modulated signals was simulated to generate a discrete spectral interference (DSI). The mathematical expression used to generate this signals is denoted by Equation (6) [23].

$$e(t) = \sum_{i=1}^{12}(c + m * sin(2\pi f_m t)) * \sin(2\pi f_i t) \tag{6}$$

Where c is the carrier amplitude, m is the modulated signal amplitude, f_m is the modulated signal frequency and f_i is the carrier frequency. In the simulations, the used parameters were: $c = 1$, $m = 0.4$, $f_m = 1$ kHz, $f_i = [0.1 - 11]$ MHz, with steps of 1 MHz between each frequency value.

A example of a simulated DSI signal added to the original train of pulses (see Fig. 9), can be visualized in Figure 10.

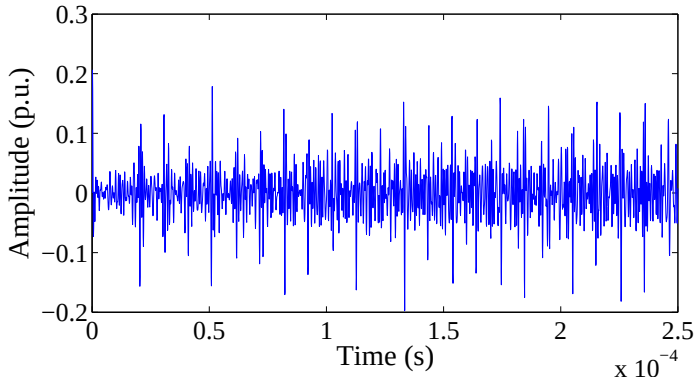

Figure 10. Simulated discrete spectral interference.

6.1.3. White-noise simulation. Other commonly interference source is the white-noise. It is defined as an uncorrelated noise process with equal power at all frequencies, as presented in Figure 11. A noise that has the same power at all frequencies in the range of $\pm\infty$ would necessarily need to have infinite power, and is therefore only a theoretical concept. However a band-limited noise process, with a flat spectrum covering the frequency range of a bandlimited communication system, is to all intents and purposes from the point of view of the system a white noise process [11]. The simulated white noise is presented in the Figure 12.

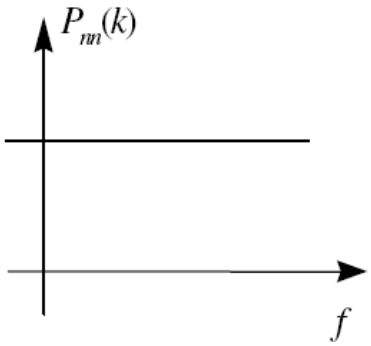

Figure 11. White noise power spectrum illustration.

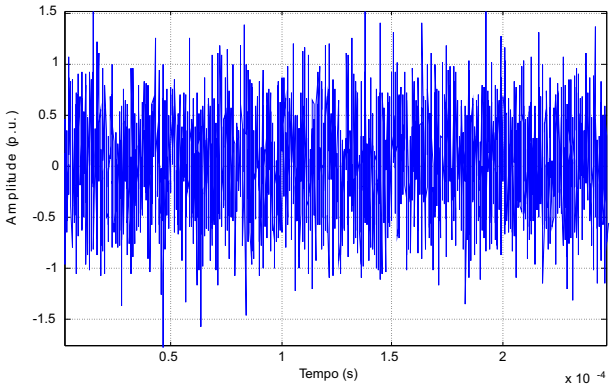

Figure 12. Simulated white noise.

After the simplified explanation about PD concepts, PD measurement methods and the main interferences sources, will be discussed the used methodologies to perform the PD measurement in HV laboratory.

7. Partial discharge measurement

7.1. Electrical partial discharge measurement

Classical measurements have been made using the LDS-6 commercial PD monitoring and diagnosis system, manufactured by the Doble Lemke Group. The DUT used in the measurements

is a 15 kV class commercial potential transformer. The LDS-6 follows closely the methodology described in [24]. It provides two separate channels for hardware gating. The suppression of external noise is achieved using a separate (gating sensor) antenna. Additional information about the LDS-6 internal architecture can be found in [24]. The measurement impedance used in the laboratory measurements was the LDM-5, also produced by Doble Lemke, and designed to match PD-signal signals above 30 MHz to a 50Ω resistive load.

7.2. HFCT partial discharge measurement

HFCT measurements have been made using the FCT-055-20:1-WB sensor from Bergoz Instrumentation. The DUT is the same potential transformer connected to a 10 kV power supply voltage and the HFCT measurements were taken concurrently with the electrical classical measurements.

8. Results

8.1. Simulated PD signals de-noise

A train of PD pulses embedded in noise and interference processes with resulting SNIR values between 3.15 dB and -42.87 dB dB has been simulated.

De-noise using the wavelet transform was done. For each resulting signal, it was calculated the cross-correlation factor (CCF) between the de-noised PD process and the original (noise-free) signal. In statistical analysis, the cross correlation factor is used to detect one particular relationship between variables. The greater the value of the CCF, the more approximate in wave shape between two variables are. Uncorrelated data sets result in an CCF of 0, whereas equivalent data sets have a CCF of 1. For this reason, the CCF can also be used as a criterion in identifying an appropriate wavelet choice for PD pulse examination [17Xma].

In the first analysis, was used a CCF equal to 0.5 (50 % of relationship) as a inferior limit for an acceptable de-noise, and was verified the correspondent SNIR value for CCF values range $\geq$ 0.5. In the sequence the mother-wavelet used in the de-noise family was systematically varied between different mother-wavelet families to verify the one that allow the biggest value of CCF. The used mother-wavelets are listed in Table 1.

DSI filtering results for each mother-wavelet are shown in Table 2. For example, using the Daubechies mother-wavelet, for a SNIR value of 3.15 dB, it was obtained a CCF of 0.97 and the "optimal" wavelet for this situation was de db2. For the situation where the calculated SNIR was -27.22 dB, the CCF value was 0.51 and the wavelet that presented the best result in this situation was the db43. The same procedure was performed using the Coiflets, Biorthogonal and Reverse Biorthogonal wavelets family.

The graphical results of the DSI noise filtering process using the Daubechies mother-wavelet is presented in Figure 13. The top trace in the figure presents the noise-free train of pulses, the middle trace is the PD pulses embedded in DSI noise and the bottom trace is the de-noised PD signal.

The same de-noise procedure was performed using the Coiflets, Biorthogonal and Reverse Biorthogonal mother-wavelets. The respective de-noise results are presented in Figures 14, 15 and 16.

The same procedure was repeated to evaluate the PD de-noise using the same mother-wavelets. In this situation, the noise free train of pulses was added to white-noise signals with different SNIR.

The obtained numerical results of this operation are presented in Table 3. Similar to DSI noise, using the Daubechies mother-wavelet, for a SNIR value of 5.94 dB, it was obtained a CCF of 0.98 and the wavelet that supplied the higher value of CCF was daub3. For the calculated SNIR equal to -10.96 dB, the CCF value was 0.66 and the wavelet that presented the best

Table 1. Wavelets used in the PD signals de-noise.

Wavelets Families	Wavelets
Daubechies	'db1' or 'haar', 'db2', ... , 'db45'.
Coiflets	'coif1', 'coif2', 'coif3', 'coif4', 'coif5'.
Biorthogonal	'bior1.1', 'bior1.3', 'bior1.5', 'bior2.2', 'bior2.4', 'bior2.6', 'bior2.8', 'bior3.1', 'bior3.3', 'bior3.5', 'bior3.7' 'bior3.9', 'bior4.4', 'bior5.5', 'bior6.8'.
Reverse Biorthogonal	'rbio1.1', 'rbio1.3', 'rbio1.5', 'rbio2.2', 'rbio2.4', 'rbio2.6', 'rbio2.8', 'rbio3.1', 'rbio3.3', 'rbio3.5', 'rbio3.7' 'rbio3.9', 'rbio4.4', 'rbio5.5', 'rbio6.8'.

Table 2. Obtained de-noise results of PD signals with DSI interference using Wavelet transform.

Mother-wavelet	Daubechies	Coiflets	Biorthogonal	Reverse Biorthogonal
SNIR (dB)	3.15 | -27.22	3.15 | -17.67	3.15 | -20.93	3.15 | -20.93
CCF	0.97 | 0.51	0.97 | 0.52	0.98 | 0.52	0.97 | 0.51
Optimal Wav.	db2| db43	coif2|coif4	bior2.6|bior3.7	rbio1.3|rbio2.8

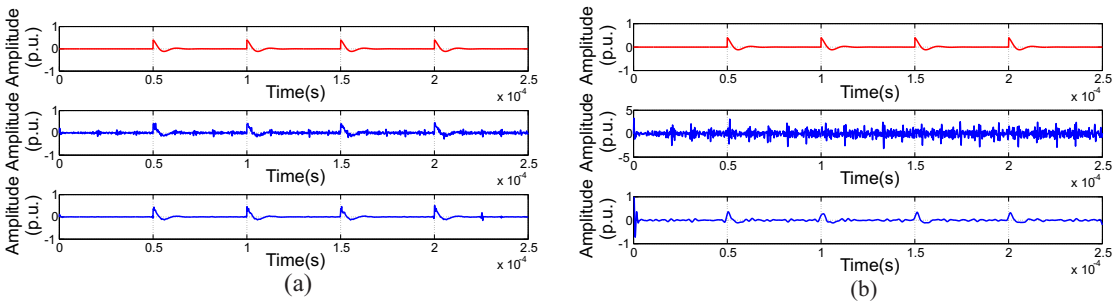

Figure 13. Denoising of a DOP-type PD event added to DSI noise using the Daubechies mother-wavelet (a) SNIR = 3.15 dB; (b) SNIR = -27.22 dB.

result in this situation was the db10. The same procedure was performed using the Coiflets, Biorthogonal and Reverse Biorthogonal wavelets family.

White-noise filtering presented a different filtering behavior when compared to DSI noise filtering. For example, for the white-noise buried signals for a SNIR equal to 0.5, the signals filtering was not visually satisfactory, and were descarted. The SNIR that supplied visual satisfactory was the same presented in Table 3.

The graphical results of the white-noise filtering are presented in Figures 17, 18, 19 and 20.

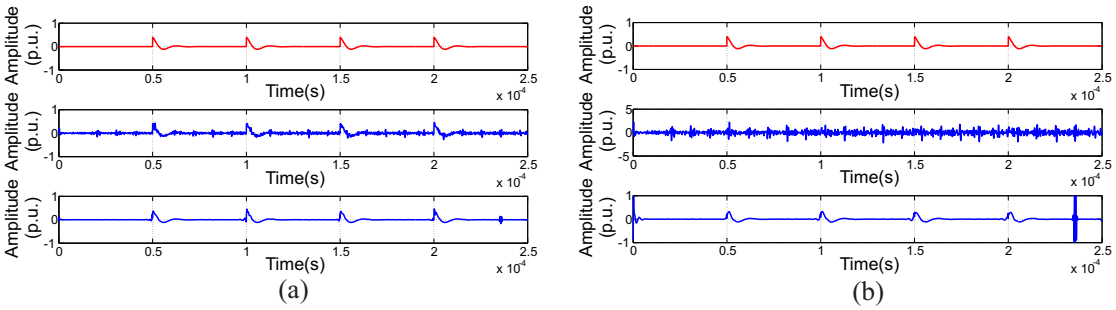

Figure 14. Denoising of a DOP-type PD event added to DSI noise using the Coiflets mother-wavelet (a) SNIR = 3.15 dB; (b) SNIR = -17.67 dB.

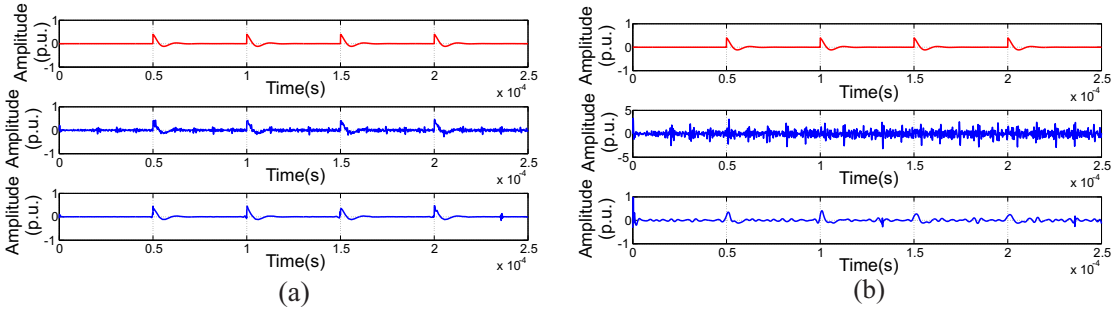

Figure 15. Denoising of a DOP-type PD event added to DSI noise using the Biorthogonal mother-wavelet (a) SNIR = 3.15 dB; (b) SNIR = -20.93 dB.

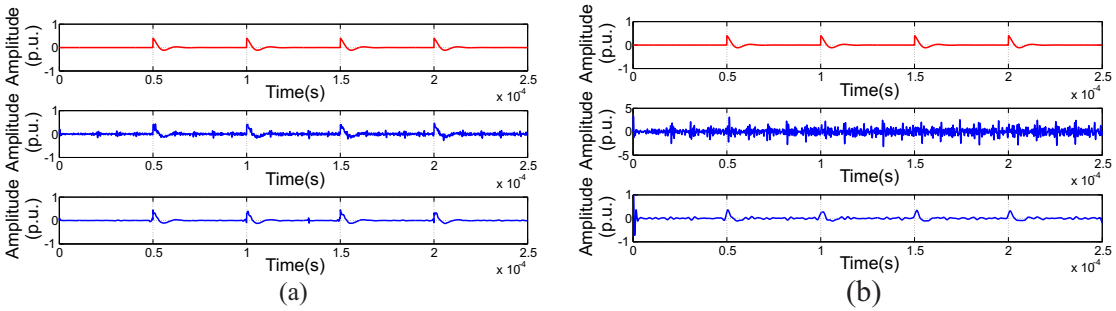

Figure 16. Denoising of a DOP-type PD event added to DSI noise using the Reverse Biorthogonal mother-wavelet (a) SNIR = 3.15 dB; (b) SNIR = -20.93 dB.

8.2. Measured PD signals de-noise

The PD measurements were performed using the techniques presented in Section 7. For the data storage, it was used a 5 GS/s Tektronix oscilloscope. The LDS-6 output was connected to channel 1, the HFCT was connected to channel 2. The measurement set-up is presented in Figure 21 . The sensitivity settings of the scope were 100 mV/div and 2 mV/div. The signals de-noise was also performed using different wavelet-mother, as presented in Table 1.

The results obtained from the measurements using the comercial PD measurement system is

Table 3. Obtained de-noise results of PD signals with white-noise interference using Wavelet transform.

Mother-wavelet	Daubechies	Coiflets	Biorthogonal	Reverse Biorthogonal
SNIR (dB)	5.94 | -10.96	5.94 | -9.62	5.94 | -13.15	5.94 | -13.14
CCF	0.98 | 0.66	0.98 | 0.71	0.99 | 0.65	0.98 | 0.61
Optimal Wav.	db3| db10	coif2|coif5	bior2.6|bior2.6	rbio4.4|rbio6.8

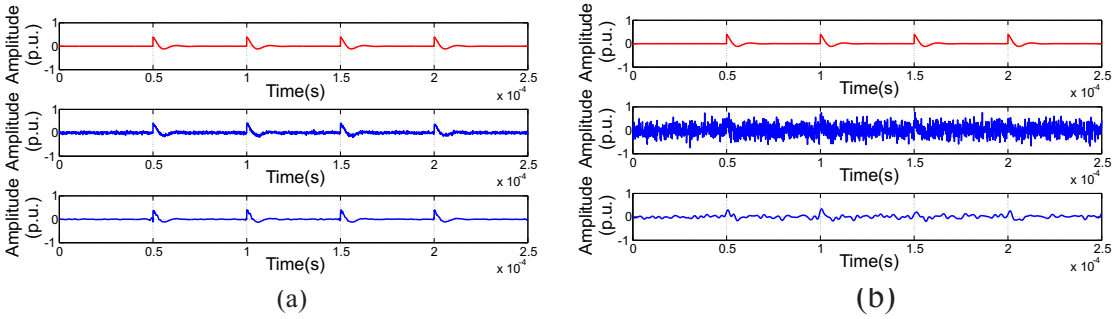

Figure 17. Denoising of a DOP-type PD event added to white-noise using the Daubechies mother-wavelet (a) SNIR = 3.15 dB; (b) SNIR = -27.22 dB.

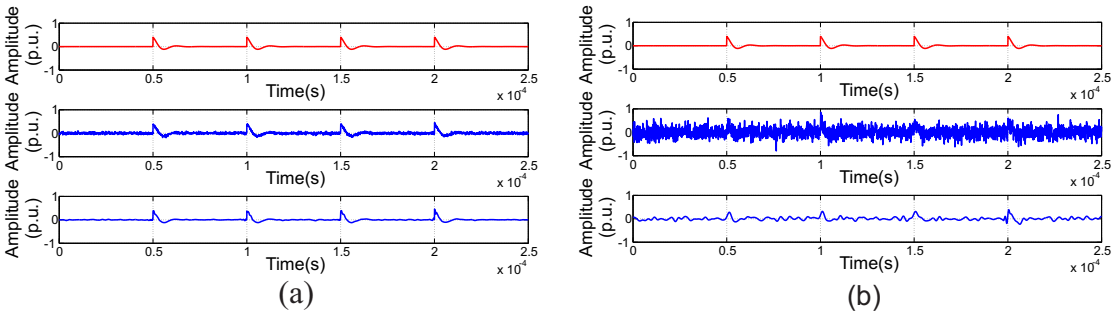

Figure 18. Denoising of a DOP-type PD event added to white-noise using the Coiflets mother-wavelet (a) SNIR = 3.15 dB; (b) SNIR = -17.67 dB.

presented in Figure 22, and the measured using the PD HCFT is presented in Figure 23.

The de-noise of the measured PD signals was satisfactory for the majority of the selected mother-wavelet. In the sequence is presented the de-noise of PD signals using the Daubechies mother-wavelet.

9. Discussion and Conclusion

Reliability of PD data gathered during on-line and on-site PD measurements is strongly influenced by external interferences. This paper presents results of the application of wavelet transform method, based on multi-resolution analysis for extracting PD pulses buried in very high levels of noise and interference.

In this paper, were generated several different signals, buried in two different sources of noise,

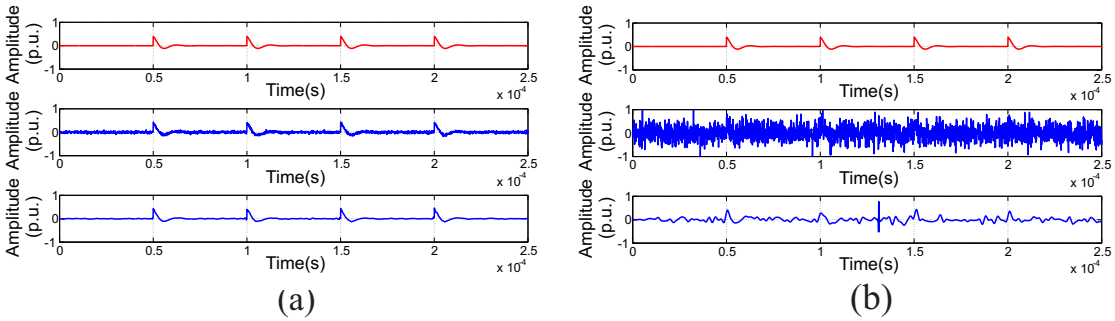

Figure 19. Denoising of a DOP-type PD event added to white-noise using the Biorthogonal mother-wavelet (a) SNIR = 3.15 dB; (b) SNIR = -20.93 dB.

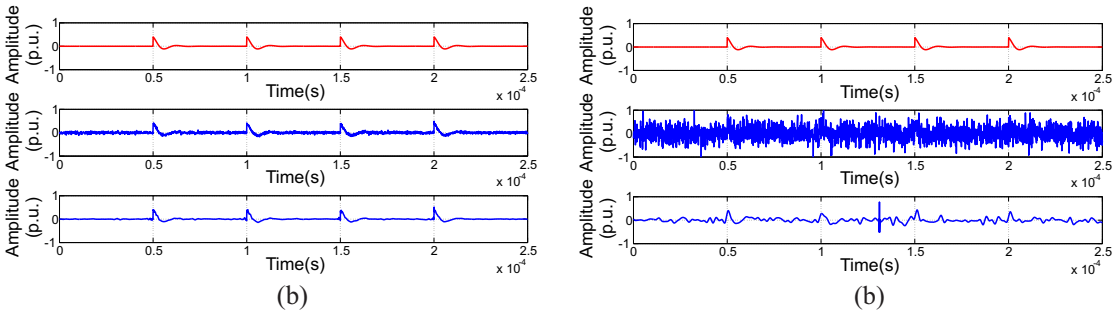

Figure 20. Denoising of a DOP-type PD event added to white-noise using the Reverse Biorthogonal mother-wavelet (a) SNIR = 3.15 dB; (b) SNIR = -20.93 dB.

Figure 21. PD measurement setup.

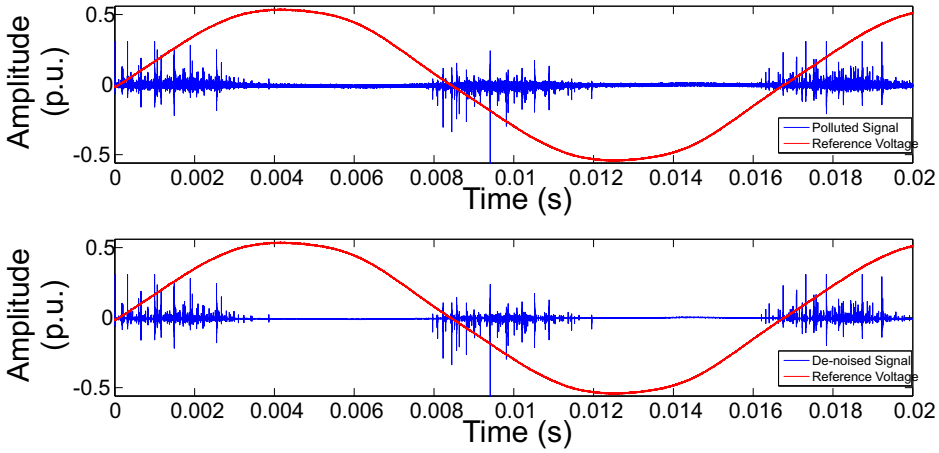

Figure 22. De-noised signal obtained from LDS-6 PD measurement.

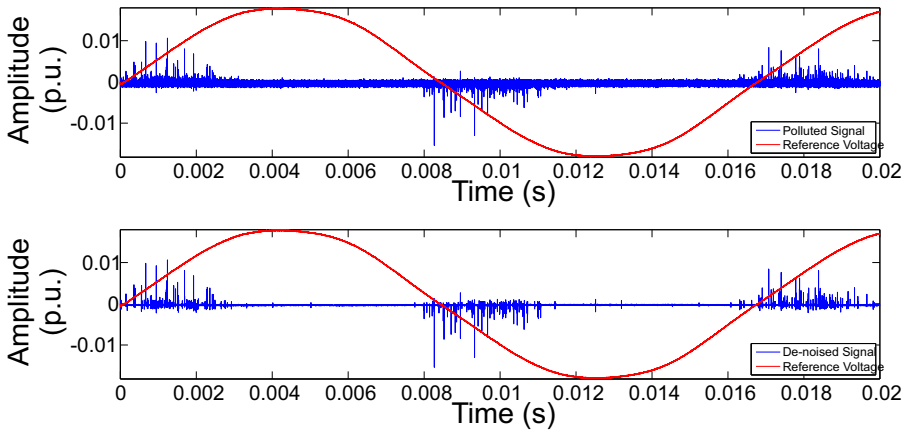

Figure 23. De-noised signal obtained using de HFCT.

the discrete spectral interference (DSI) and the white-noise, often encountered during on-line on-line and on-site PD tests and measurements.

To use wavelet theory for PD analysis, it is vital to select the appropriated wavelet and this is determined by the nature of the PD pulse. The cross-correlation factor between the de-noised signal and the original (noise-free) signal ca be used as an efficient criterion to evaluate the optimal wavelet for the measured PD pulse. For the signals measured using a RLC coupling device, it was observed that the wavelets of higher order are the most appropriated.

It was observed that the DSI noise, because its fixed frequency range, was easier to be filtered than the white-noise, that presents frequency components in all frequency spectrum. Based on the obtained results, it was observed that denoising problems can be solved using the wavelet transform.

Further tests on practical PD data in on-site measurements will be performed to also estimates the apparent charge of PD pulses.

References

[1] Nattrass D A 1988 *IEEE Electrical Insulation Magazine* **4** 10–23
[2] Satish L and Nazneent B 2003 *IEEE Transactions on Dieletrics and Electrical Insulation* **10** 354–367
[3] IEC 60270 2000 High-voltage test techniques - partial discharge measurements Tech. rep. Geneve, Switzerland
[4] Shim I and Soraghan J 2000 *IEEE Electrical Insulation Magazine* **16** 6 – 12
[5] Cigre 1993 Partial discharge detection by means of acoustic detection Tech. rep. USA
[6] Judd M, Cleary G and ci Bennoch 2002 *IEEE Power Engineering Review* **22** 57–58
[7] Michel M 2007 *19th International Conference on Electricity Distribution* 1–4
[8] Moore P J, Portugues I E and Glover I A 2003 *Power Engineering Society General Meeting* **2**
[9] Ma X, Zhou C and Kemp I 2002 *IEEE Electrical Insulation Magazine* **18** 37–44
[10] Hao L, LLewin P and Swingler S 2008 *International Conference on Condition Monitoring and Diagnosis* 21–24
[11] Vaseghi S V 2000 *Advanced Digital Signal Processing and Noise Reduction* (England: John Wiley e Sons Ltd)
[12] Zang H, Blackburn T, BTPhung and DSen 2007 *IEEE Transactions on Dieletrics and Electrical Insulation* **14** 3–14
[13] Feser K, Konig G, Ott J and Setiz P 1988 *IEEE International Symposium of Electrical Insulation* **73**
[14] Borsi H, Gackenbach E and Schichler U 1993 *8th Intern. Sympos. HV Engineering, Yokohama, Japan*
[15] Zang H, Blackburn T R, Phung B T and Liu Z 2004 *International Conference on Power System Technology*
[16] Zhang Z S and Xiao D M 2008 *Transactions on Circuits and Systems* **7**
[17] Sriram S, Nitin S, Prabhu K M M and Bastiaans M J 2005 *IEEE Transactions on Dielectrics and Electrical Insulation* **12** 1182 – 1191
[18] ZhaoHeng D, ShangHe L and Lei W 2010 *International Conference on Signal Processing Systems*
[19] SMatsumoto, YShibuya and ROgura 2011 *XVII International Symposium on High Voltage Engineering* (Hannover, Germany)
[20] Burrus C S 1998 *Introduction to Wavelets Transforms* (EUA: Prentice- Hall)
[21] Vidya H A, Krishnan V and Mallikarjunappa K 2008 *International Conference on Condition Monitoring and Diagnosis*
[22] Lathi B P 1998 *Modern Digital and Analog Communications Systems* - (USA: Oxford University Press)
[23] Zhou X, Zhou C and Kemp I J 2005 *IEEE Transactions on Dielectrics and Electrical Insulation* **12**
[24] DRusswurm 2000 *HV Testing, Monitoring and Diagnostic Workshop* (Alexandria, Virginia)
[25] GKeppel and SZedeck 1989 *Data Analysis for Research Designs - Analysis of Variance and Multiple Regression/Correlation Approaches* (New York, USA: W. H. Freeman and Company)